Hepatitis B reactivation during glioblastoma treatment with temozolomide: A cautionary note

M.G. Chheda, MD; J. Drappatz, MD; N.J. Greenberger, MD; S. Kesari, MD, PhD; S.E. Weiss, MD; D.C. Gigas, RN; L.M. Doherty, RN, NP; and P.Y. Wen, MD

We diagnosed a 50-year-old right-handed Chinese man with a right temporal glioblastoma in October 2005, after he presented with headaches and progressive left hemiparesis. He had no significant past medical illnesses and no known history of hepatitis, blood transfusion, or IV drug use. He had immigrated to the United States 5 years previously from Shanxi Province, China. He had a craniotomy with gross total tumor resection. He was discharged on rapid dexamethasone taper beginning at 24 mg total a day; 2.5 weeks later, he was on dexamethasone 4 mg total a day.

Three weeks postresection, he began radiotherapy (60 Gy in 30 fractions over 6 weeks) together with 6 weeks of daily temozolomide (75 mg/m^2/day). Liver function tests (LFTs) were normal just prior to chemotherapy and radiation, except an SGPT 68 U/L (normal 7 to 56 U/L) (figure). During chemo-radiation therapy, the nadir of white blood cell count was 5.3 K/μL, absolute neutrophil count 3.89 K/μL, and absolute lymphocyte count 0.58 K/μL. Throughout chemo-radiation, his dexamethasone continued at 4 mg total a day; thereafter he tapered down to 0.5 mg total a day. One week post-radiation, he developed worsening left hemiparesis as a result of a subdural collection. His dexamethasone dose was briefly increased from 0.5 mg daily to 2 mg daily. We noticed elevated LFTs (figure).

From Division of Cancer Neurology, Department of Neurology, Brigham and Women's Hospital (M.G.C., J.D., S.K., P.Y.W.); Center for Neuro-Oncology (M.G.C., J.D., S.K., D.C.G., L.M.D., P.Y.W.) and Department of Radiation Oncology (S.E.W.), Dana-Farber Cancer Institute/Brigham and Women's Cancer Center; Division of Gastroenterology, Brigham and Women's Hospital (N.J.G.) and Harvard Medical School, Boston, MA.

Disclosure: The authors report no conflicts of interest.

Received June 27, 2006.

Accepted in final form November 21, 2006.

Address correspondence and reprint requests to Dr. Milan G. Chheda, Dana-Farber Cancer Institute, Shields Warren 430 D, 44 Binney Street, Boston, MA 02115; e-mail: mchheda@partners.org

One week later, 5 weeks after completing temozolomide, he was admitted with worsening liver tests (figure). Hepatitis B viral DNA was 724,000 copies/mL and HBeAb was positive. Alpha fetoprotein was 5 IU/mL (normal 0 to 7.4 IU/mL). His medications were tolterodine, levetiracetam, and atovaquone (dexamethasone had been tapered off). Examination revealed a jaundiced man with a mildly enlarged liver. There was no asterixis or encephalopathy. We started the antiviral agent lamivudine 100 mg daily and liver tests improved over the next 7 weeks (figure). Hepatitis B viral DNA reached 797,000 copies/mL before returning to <200 copies/mL.

Three months after completion of radiotherapy with concomitant temozolomide, he began treatment with adjuvant temozolomide at 150 mg/m^2 daily for 5 days/28 days while continuing on lamivudine. He received two cycles of therapy, the second of which was at 175 mg/m^2 daily for 5 days/28 days, with no further elevation in LFTs. He developed multiple drop metastases in the spine. We discontinued temozolomide and administered palliative radiotherapy, together with lomustine and erlotinib.

Discussion. Worldwide, an estimated 350 million people are chronic hepatitis B carriers, with approximately 170 million carriers in China and 1.25 million in the United States, most of whom are asymptomatic.[1] Immunosuppressive cytotoxic chemotherapy increases the risk for hepatitis B reactivation, especially in patients with lymphoma or breast cancer, those with detectable pre-chemotherapy HBV DNA load, or whose treatment includes corticosteroids or anthracyclines.[2,3] Prophylactic lamivudine during and for 6 months after treatment has been safely administered in hepatitis B carriers with predominantly hematologic malignancies and should be considered in cancer patients who are carriers.[4,5]

We describe a case of hepatitis B reactivation in a man with glioblastoma who received radiotherapy with concomitant temozolomide and low-dose corticosteroids. The relatively unremarkable liver tests on October 28, 2005, and subsequent positive tests for HBsAg, HbcAb IgG, and HBeAb indicated the patient was an inactive hepatitis B carrier. Chemotherapy is known to activate hepatitis B in cancer patients. Since his steroid dose was low, it is likely the immunosuppression from temozolomide played the predominant role in viral reactivation; however, we cannot be completely certain that steroids had no role in our particular case. There are two putative mechanisms of hepatitis B virus reactivation during chemotherapy: immunosuppression from chemother-

	10/28/05[a]	12/8/05[a]	1/17/06[a]	1/26/06[a]	1/29/06[b]	2/28/06[b]	3/16/06[a]	5/26/06	6/6/06[a]
Serum bilirubin (mg/dL)	0.2	0.4	1	2.9	3.1	0.9	0.5		0.7
SGOT (U/L)	38	63	298	1728	1053	159	39		29
SGPT (U/L)	68	159	915	2716	1679	201	36		64
Alkaline phosphatase (U/L)	78	58	74	109	87	66	58		65
Hepatitis B surface antigen (HBsAg)			(+)						
Hepatitis B surface antibody (HBsAb)			(-)						
Hepatitis B core antibody (HBcAb IgG)			(+)						
Hepatitis B viral DNA (copies/mL)				724,000		797,000	<200	<40	
Hepatitis B e antibody (HBeAb)					(+)				
Hepatitis C antibody (HCVAb)			(-)						

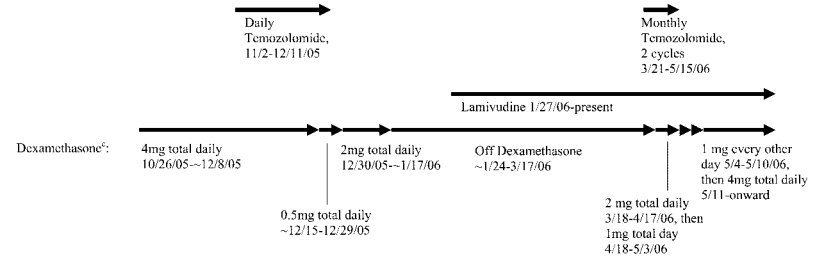

Figure. Liver function test trend with respect to temozolomide chemotherapy and lamivudine treatment. [a] Normal ranges for the Dana-Farber Cancer Institute laboratory are as follows: serum bilirubin 0.2 to 1.3 mg/dL, SGOT 14 to 46 U/L, SGPT 7 to 56 U/L, alkaline phosphatase 38 to 126 U/L. [b] Normal ranges for the Brigham and Women's Hospital laboratory are as follows: serum bilirubin 0.2 to 1.2 mg/dL, SGOT 9 to 30 U/L, SGPT 7 to 52 U/L, alkaline phosphatase 36 to 118 U/L. [c] When dexamethasone dates have a ~ symbol, it indicates that steroids were changed over several days to the noted dose.

apy enhances virus replication leading to hepatic toxicity; or chemotherapy-induced T-cell depletion dampens host response to viral antigens and allows broader hepatocyte infection. When the chemotherapy is withdrawn (in our case, at the end of the 6 weeks of temozolomide), the rebound immune response causes hepatocyte destruction.[6]

Since 2005, the standard treatment for glioblastoma has been radiotherapy with 6 weeks of daily low-dose concomitant temozolomide, followed by 6 months of adjuvant temozolomide.[7] Prolonged daily temozolomide dosing is associated with lymphopenia and an increased risk of opportunistic infections such as *Pneumocystis pneumonia*. Although reactivation of hepatitis B infection has not been reported previously in patients with brain tumor undergoing chemotherapy, the widespread use of prolonged daily dosing of temozolomide is likely to increase the incidence of this complication. To avoid this, patients at risk of hepatitis B—either those who come from endemic areas or those who have high-risk behaviors—should be considered for hepatitis B screening prior to initiating temozolomide chemotherapy. If the test for hepatitis B DNA reveals elevated levels, patients should receive prophylactic therapy with agents such as lamivudine, adefovir, or entecavir—all active against hepatitis B—for at least 2 months after chemotherapy. Finally, in chemotherapy patients with elevated LFTs, physicians should include viral hepatitis in the differential diagnosis, along with medication-induced hepatotoxicity.

References

1. Sun Z, Ming L, Zhu X, Lu J. Prevention and control of hepatitis B in China. *J Med Virol* 2002;67:447–450.
2. Law JK, Ho JK, Hoskins PJ, Erb SR, Steinbrecher UP, Yoshida EM. Fatal reactivation of hepatitis B post-chemotherapy for lymphoma in a hepatitis B surface antigen-negative, hepatitis B core antibody-positive patient: potential implications for future prophylaxis recommendations. *Leuk Lymphoma* 2005;46:1085–1089.
3. Yeo W, Zee B, Zhong S, et al. Comprehensive analysis of risk factors associating with hepatitis B virus (HBV) reactivation in cancer patients undergoing cytotoxic chemotherapy. *Br J Cancer* 2004;90:1306–1311.
4. Lok AS, McMahon BJ, Practice Guidelines Committee, American Association for the Study of Liver Diseases (AASLD). Chronic hepatitis B: update of recommendations. *Hepatology* 2004;39:857–861.
5. Yeo W, Chan PK, Ho WM, et al. Lamivudine for the prevention of hepatitis B virus reactivation in hepatitis B s-antigen seropositive cancer patients undergoing cytotoxic chemotherapy. *J Clin Oncol* 2004;22:927–934.
6. Yeo W, Chan PK, Zhong S, et al. Frequency of hepatitis B virus reactivation in cancer patients undergoing cytotoxic chemotherapy: a prospective study of 626 patients with identification of risk factors. *J Med Virol* 2000;62:299–307.
7. Stupp R, Mason WP, van den Bent MJ, et al. Radiotherapy plus concomitant and adjuvant temozolomide for glioblastoma. *N Engl J Med* 2005;:987–996.

VIDEO Periodic alternating nystagmus in isolated nodular infarction

H.-S. Jeong, MD; J.Y. Oh, MD; J.S. Kim, MD; J. Kim, MD; A.Y. Lee, MD; and S.-Y. Oh, MD

Periodic alternating nystagmus (PAN) is characterized by periodic reversal of horizontal jerky nystagmus with a null period of several seconds. Damage to the uvulonodulus or to their connections with the brainstem vestibular nuclei has been suggested as a mechanism of PAN.[1,2] However, PAN has rarely been reported in circumscribed cerebellar lesion.[3]

We report a patient with isolated nodular infarction who developed PAN without fixation in association with perverted head-shaking nystagmus (HSN) and loss of tilt suppression of the postrotatory nystagmus. This is the first report of PAN in circumscribed cerebellar infarction, and provides further evidence that PAN occurs due to dysfunction of cerebellar nodulus.

Additional material related to this article can be found on the *Neurology* Web site. Go to www.neurology.org and scroll down the Table of Contents for the March 20 issue to find the title link for this article.

Case report. A 69-year-old man with a history of hypertension developed acute vertigo with nausea/vomiting and postural imbalance. On examination, we observed spontaneous horizontal nystagmus in the primary position which reversed its direction with a cycle of approximately 2 minutes and a transition period of several seconds by using video Frenzel goggles (SLMED, Seoul, Korea) (see the video on the *Neurology* Web site at www.neurology.org). The horizontal nystagmus remained in up- and down-gazes with decreased amplitude. Periodic head turn was not observed. With fixation, the nystagmus disappeared. Downbeat nystagmus was induced for about 10 seconds by horizontal head-shaking for 20 seconds (video). Gaze-evoked nystagmus or saccadic dysmetria was not observed. Horizontal and vertical smooth pursuit appeared to be normal for his age. Horizontal head thrust tests were normal. His gait was ataxic, but no limb dysmetria was present on finger-to-nose and heel-to-shin test.

Somatosensory and brainstem auditory evoked potentials and audiogram were normal. Bithermal caloric tests showed symmetric responses. Sinusoidal harmonic accelerations (peak velocity: 50 °/second, frequency range: 0.02 to 0.32 Hz) showed normal gains and phases of the vestibulo-ocular reflex (VOR). Time constants (TCs) of the per- and postrotatory nystagmus during step velocity rotations (peak velocity: 100 °/second, acceleration and deceleration: 100 °/second^2, duration: 60 seconds) were mildly increased at 18.3 seconds (normal: 14.7 seconds) and TCs of the postrotatory nystagmus were not suppressed by forward head tilt (mean: 18.0 seconds). Diffusion-

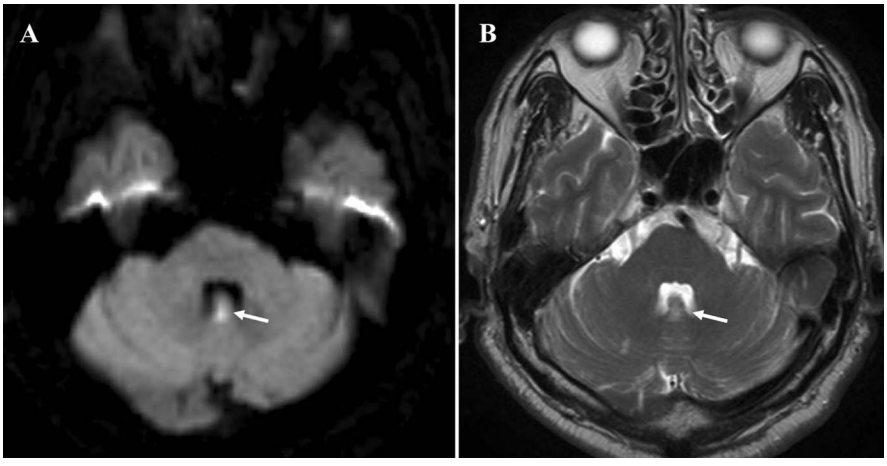

Figure. Diffusion-weighted (A) and T2-weighted imaging (B) of MR shows an acute infarction restricted to the cerebellar nodulus.

weighted MRI disclosed a circumscribed acute infarction in the cerebellar nodulus (figure). Other parts of the cerebellum and the brainstem were intact. Over the following several days, vertigo, PAN, and postural imbalance resolved.

Discussion. We observed PAN, perverted HSN, and impaired tilt suppression of the postrotatory nystagmus in a patient with isolated nodulus infarction. In monkeys, ablation of the cerebellar nodulus gave rise to PAN in darkness.[4] Since the nodulus normally inhibit the time course of rotationally induced nystagmus, i.e., the velocity storage mechanism, PAN has been ascribed to prolonged vestibular response after uvulonodular damage, and reversal of the nystagmus by normal vestibular repair mechanism, which would result in periodic oscillation of PAN.[1,4]

The postrotatory nystagmus is normally suppressed by head tilting just after cessation of step-velocity rotation (tilt suppression). This suppressive effect is lost after ablation of the uvulonodulus.[4,5] Indeed, in our patient, TCs of the per- and postrotatory nystagmus were mildly increased to an average of 18.3 seconds. Furthermore, TCs of the postrotatory nystagmus were not diminished by head tilt after step velocity rotation.

In vestibulopathies, HSN can be induced by head oscillation at 2 Hz for approximately 20 seconds.[1] In perverted HSN, HSN develops in another plane than that being stimulated by head oscillation. Perverted HSN is explained by abnormal cross-coupling of vestibular responses that have usually been attributed to lesions in the central vestibular pathways, including the vestibulocerebellum.[4,6] The uvulonodulus are also known to control spatial orientation of the angular VOR and may participate in cross-coupling of the velocity storage during head tilt.[4] Damage to these areas may induce abnormal activation of the cross-coupling during head oscillation and result in perverted HSN.[4]

In our patient, PAN was present only without visual fixation. However, most of the previously reported cases of PAN showed little effect of visual fixation on the nystagmus. Cerebellar flocculus is important for suppression of vestibular nystagmus by visual fixation,[7] and the disappearance of PAN with visual fixation in our patient suggests intact floccular function. The absence of saccadic dysmetria, gaze-evoked nystagmus, and spontaneous downbeat nystagmus in our patient is also consistent with the integrity of the oculomotor vermis and floccular region, and is suggestive of isolated nodular dysfunction.

Previously, multiple cerebellar and brainstem lesions or diffuse cerebellar atrophy have been reported with PAN.[2,3] However, despite the numerous reports on nodular dysfunction as a mechanism of PAN, pathologic or radiologic confirmation of circumscribed nodular lesions has been unavailable in patients with PAN. The PAN and associated findings in our patient with isolated nodular infarction provide further evidence that PAN develops due to nodular dysfunction.

From the Department of Neurology (H.-S.J., J.Y.O., J.K., A.Y.L., S.-Y.O.), Chungnam National University College of Medicine; and Department of Neurology (J.S.K.), Seoul National University College of Medicine, Korea.

Disclosure: The authors report no conflicts of interest.

Received October 10, 2006. Accepted in final form November 27, 2006.

Address correspondence and reprint requests to Dr. Sun-Young Oh, Department of Neurology, Chungnam University Hospitals 640, Daesa-dong, Junggu, Daejeon, 301-721, Korea; e-mail: ohsun@medigate.net

References

1. Leigh RJ, Zee DS. The neurology of eye movements. New York: Oxford Univ Press, 2006.
2. Furman JM, Wall C 3rd, Pang DL. Vestibular function in periodic alternating nystagmus. Brain 1990;113:1425–1439.
3. Oh YM, Choi KD, Oh SY, Kim JS. Periodic alternating nystagmus with circumscribed nodular lesion. Neurology 2006;67:399.
4. Sheliga BM, Yakushin SB, Silvers A, Raphan T, Cohen B. Control of spatial orientation of the angular vestibulo-ocular reflex by the nodulus and uvula of the vestibulocerebellum. Ann NY Acad Sci 1999;871:94–122.
5. Hain TC, Zee DS, Maria BL. Tilt suppression of vestibulo-ocular reflex in patients with cerebellar lesions. Acta Otolaryngol 1988;105:13–20.
6. Kim JS, Ahn KW, Moon SY, Choi KD, Park SH, Koo JW. Isolated perverted head-shaking nystagmus in focal cerebellar infarction. Neurology 2005;64:575–576.
7. Waespe W, Cohen B, Raphan T. Role of the flocculus and paraflocculus in optokinetic nystagmus and visual-vestibular interactions: effects of lesions. Exp Brain Res 1983;50:9–33.

Treatment-responsive pudendal dysfunction in chronic inflammatory demyelinating polyneuropathy

L. Bussemaker, MD; H.J. Schelhaas, MD, PhD; S. Overeem, MD, PhD; W.P.M. Hopman, MD, PhD; and M.J. Zwarts, MD, PhD

A 48-year-old man presented with sensory disturbances in both hands and feet and difficulties when opening bottles or climbing the stairs. His symptoms had developed over 2 weeks and were preceded by fever of unknown origin. There was no history of toxin exposure. His past medical history was remarkable for Henoch–Schonlein purpura with nephritis and intestinal necrosis. Examination showed weakness of the neck, arm, and proximal leg muscles (Medical Research Council [MRC] grade 4). Vibration sense was diminished in both hands and feet, without a sensory level. Tendon reflexes were absent. There were no gastrointestinal symptoms, purpurae, or evidence of glomerulonephritis. Nerve conduction studies showed that the distal motor latency (DML) was increased in the median (5.6 milliseconds), ulnar (5.4 milliseconds), and peroneal nerves (19.2 milliseconds) and that the nerve conduction velocity (NCV) was decreased in the median (32 m/s) and peroneal (15.5 milliseconds) nerves, with conduction block and sural sparing.[1] The CSF was normal. Screening for syphilis was negative. The patient was diagnosed with Guillain–Barré syndrome (GBS) and was treated with IV gammaglobulin (IVIG; 0.4 g/kg daily for 5 days), which led to almost complete resolution of the muscle weakness within 3 weeks. Four weeks after discharge, the patient was readmitted with similar but more severe symptoms. In addition, he now reported fecal incontinence and a diminished sense of stool passage. He also complained about new-onset erectile dysfunction, but urinary function was normal. There were no additional signs or symptoms of autonomic dysfunction. There was weakness of both arms and legs (MRC grade 3 to 4), absent distal vibration sense, and no tendon reflexes. Perianal sensation was normal, but voluntary sphincter contraction was nearly abolished. Nerve conduction studies showed an increased DML and a reduced NCV in the median, ulnar, and peroneal nerves, with conduction block in the median nerve. There were no sural sensory nerve action potentials or ulnar F-responses. Concentric needle electromyography (EMG) of the external anal sphincter revealed a reduced recruitment pattern both at rest and during maximum contraction, without fibrillation potentials or positive sharp waves. Lumbosacral magnetic stimulation showed an increased latency over the left pudendal nerve (20 milliseconds) and no response on the right. MRI of the lumbar spine was normal; nerve biopsy was not performed.

Anal manometry[2] revealed a decreased resting pressure of the internal sphincter (32 mm Hg; normal ± 2 SD 66 ± 46 mm Hg) and a decreased maximal squeeze pressure (a combination of internal and external sphincter function; 57 mm Hg vs normal 218 ± 140 mm Hg; figure). As a result, the maximal squeeze increment was diminished (35 mm Hg; normal 90 ± 64 mm Hg), indicating impaired voluntary contraction of the external sphincter. Rectal sensitivity to balloon distension was not affected.

Under the revised diagnosis of chronic inflammatory demyelinating polyneuropathy (CIDP), the patient was again treated with IVIG. Three weeks later, muscle strength had increased, fecal continence had improved, and erectile function had returned to normal. Anal manometry showed a significant increase in resting pressure (to 51 mm Hg), maximal squeeze pressure (to 106 mm Hg), and maximal squeeze increment (to 80 mm Hg; figure). This was accompanied by an increase in NCV and a nearly normalized recruitment pattern on needle EMG. After 10 months, the patient had made a nearly full recovery: He was continent and had only some residual numbness in the feet with minimal toe weakness (MRC 4+). Nerve conduction studies still showed prolonged DMLs and reduced NCVs, compatible with the diagnosis of CIDP.[3,4]

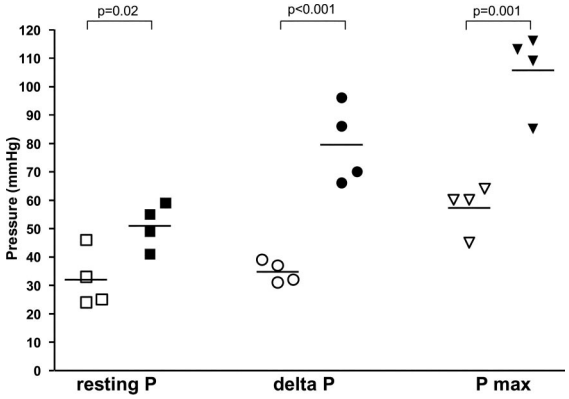

Figure. Results of anal manometry obtained with a standard station-pull-through technique with a water-perfused catheter and radially oriented recording points.[2] Resting and squeeze pressures in the anal canal were measured at consecutive 1-cm levels in four separate quadrants. The highest resting pressure (resting P), maximal squeeze pressure (P max; maximal pressure in the anal canal during squeezing), and maximal squeeze increment (delta P; increase of pressure over resting pressure during squeezing) recorded in each quadrant are depicted together with their average values. The open symbols represent values before treatment with IV gammaglobulin and filled symbols values after treatment. Differences before and after treatment were tested for statistical significance with Student t test.

Discussion. Our case shows that fecal incontinence caused by bilateral demyelinization of the pudendal nerve can be part of the clinical spectrum of CIDP. The onset, course, and response to treatment paralleled the course of the motor and sensory symptoms. Furthermore, the EMG findings could only be explained by a demyelinating disorder.

Prior to nerve conduction studies and anorectal manometry, autonomic failure was considered the most likely cause of the patient's incontinence.[5] However, although autonomic dysfunction is often pronounced in GBS,[6] it is typically mild in CIDP.[7] Moreover, both the EMG studies and the anal manometry clearly pointed to the involvement of voluntary anal function. In the past, "unequivocal incontinence" was considered an exclusion criterion for CIDP.[4] Although it is rare, fecal incontinence can be present, and patients should be questioned about it. If not, this treatable symptom may not be mentioned voluntarily by patients and certainly will not be picked up on routine nerve conduction studies.

From the Departments of Neurology (L.B., H.J.S., S.O.), Clinical Neurophysiology (S.O., M.J.Z.), and Gastroenterology (W.P.M.H.), Radboud University Nijmegen Medical Center, the Netherlands.

Disclosure: The authors report no conflicts of interest.

Received September 16, 2006. Accepted in final form November 27, 2006.

Address correspondence and reprint requests to Dr. H.J. Schelhaas, Department of Neurology (HP 935), Radboud University Nijmegen Medical Center, PO Box 9101, 6500 HB Nijmegen, the Netherlands; e-mail: H.Schelhaas@neuro.umcn.nl

References

1. Bansal R, Kalita J, Misra UK. Pattern of sensory conduction in Guillain–Barre syndrome. Electromyogr Clin Neurophysiol 2001;41:433–437.
2. Bharucha AE. Update of tests of colon and rectal structure and function. J Clin Gastroenterol 2006;40:96–103.
3. Franssen H, Vermeulen M, Jennekens FGI. Chronic inflammatory neuropathy. In: Emery A, ed. Diagnostic criteria of neuromuscular diseases. London: Royal Society of Medicine Press, 1997:53–56.
4. Ad Hoc Subcommittee of the American Academy of Neurology AIDS Task Force. Research criteria for diagnosis of chronic inflammatory demyelinating polyneuropathy (CIDP). Neurology 1991;41:617–618.
5. Rao SS. Pathophysiology of adult fecal incontinence. Gastroenterology 2004;126:S14–S22.
6. Lichtenfeld P. Autonomic dysfunction in the Guillain–Barre syndrome. Am J Med 1971;50:772–780.
7. Stamboulis E, Katsaros N, Koutsis G, et al. Clinical and subclinical autonomic dysfunction in chronic inflammatory demyelinating polyradiculoneuropathy. Muscle Nerve 2006;33:78–84.

Multiple sclerosis: Relating MxA transcription to anti-interferon-β-neutralizing antibodies

L.A. Hoffmann, MD; M. Krumbholz, MD; H. Faber; T. Kuempfel, MD; M. Starck, MD; W. Pöllmann, MD; E. Meinl, MD; and R. Hohlfeld, MD

Interferon-β (IFNβ) treatment in multiple sclerosis (MS) induces neutralizing antibodies (NAB) in 10 to 30% of patients.[1,2] NAB are associated with a reduction of bioactivity of IFNβ, and have a negative impact on therapeutic response.[3] Analysis of IFNβ-inducible genes is a direct and practical approach to monitor therapy.[4,5] The expression of three IFNβ-induced genes in antibody-positive patients with MS was recently analyzed.[6] We performed a similar study to evaluate the relationship between the expression of myxovirus resistance protein A (MxA) and NAB activity. Our results confirm and extend previously reported results.[6]

Methods. We collected serum and PAXgene (PreAnalytiX/Qiagen, Hilden, Germany) samples from 81 patients with relapsing-remitting MS (RR-MS) (54 women, 27 men, median age 38, Expanded Disability Status Scale [EDSS] median 2.0, range 0 to 6.5) before (n = 62) and 12 to 24 hours after (n = 71) injection of IFNβ (Avonex, n = 12; Rebif, 3 × 22 μg, n = 13; Rebif, 3 × 44 μg, n = 39; Betaferon, n = 17). Treatment duration was >6 months in all cases. We also collected blood samples from 25 untreated control patients with RR-MS (19 women, 6 men, median age 32 years, EDSS median 2.0, range 0.0 to 5.0). We analyzed transcription of MxA and glyceraldehyde-3-phosphate dehydrogenase (GAPDH) as housekeeping gene by TaqMan PCR (ABI 7300, ABI, Darmstadt, Germany). We used the following MxA primers and probes: forward 5′-GAGGAGATCTTTCAGCACCTGATG-3′, reverse 5′-GTACGTCTGGAGCATGAAGAACTG-3′, probe Fam-TCACCAGGAGGCCAGCAAGCG-Tamra (exon 19-20), and for GAPDH as suggested by ABI. NAB analysis was performed at BioMonitor (Copenhagen, Denmark) using a previously described cytopathic effect assay (CPE), which measures the ability of NAB to counteract the protective effect of IFNβ when cultured human A549 cells (subclone MC-5) are exposed to a cytopathic IFNβ-sensitive virus (encephalomyocarditis virus). Results are reported as neutralizing capacity (NC), which represents the percentage of the added IFNβ (10 LU/mL) neutralized by the serum (5% v/v).[7] All samples were tested for endogenous cytotoxicity and intrinsic antiviral activity. NC below 20% was regarded as negative, 20 to 79% as low positive, and 80% or above as high positive. The laboratory workers who performed the NAB assays were blinded with respect to the MxA transcription data, and vice versa.

Results. Within a time frame of 12 to 48 hours, pilot experiments (data not shown) showed maximum MxA transcription at 12 hours, with a moderate decrease at 24 hours postinjection (about 50 to 80% of the 12-hour values). At 24 to 48 hours MxA transcription further decreased, but was still above the basal levels observed in untreated MS and control subjects. Blood sampling before 12 hours postinjection is inconvenient for clinical routine purposes, as injections are usually given in the evening. Therefore

Additional material related to this article can be found on the *Neurology* Web site. Go to www.neurology.org and scroll down the Table of Contents for the March 20 issue to find the title link for this article.

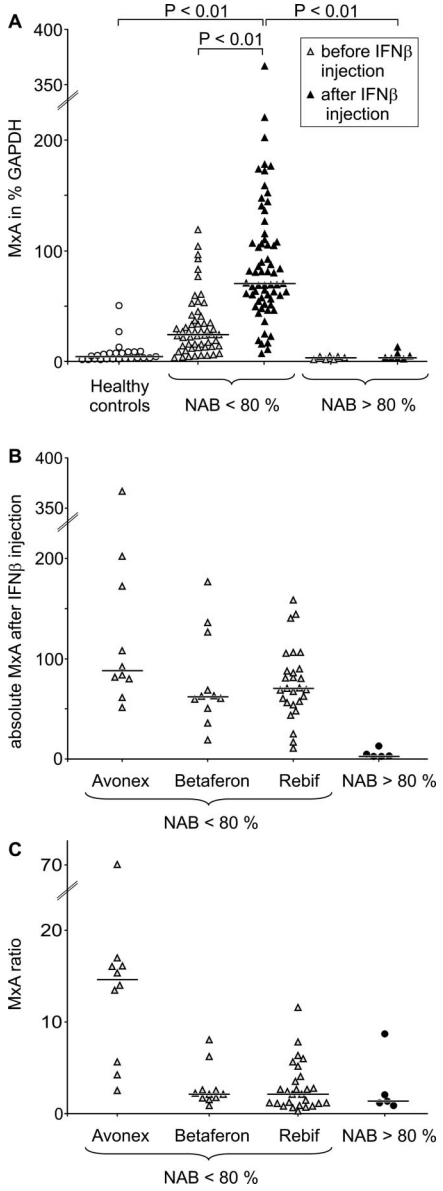

Figure. (A) Induction of myxovirus resistance protein A (MxA) mRNA by interferon-β (IFNβ) therapy in vivo in neutralizing antibodies (NAB)$^{neg/low}$ patients, but not in NAB^{high} patients. Expression of MxA as percentage of the housekeeping gene GAPDH was analyzed for untreated controls (median MxA 4% GAPDH), patients with negative or low neutralizing antibodies (NAB$^{neg/low}$) before (median MxA 24%) and 12 to 24 hours after (median MxA 71%) IFNβ injection, and patients with high NAB activity (NAB^{high}) before (median MxA 3%) and 12 to 24 hours after (median MxA 4%) IFNβ injection. The results show a significant (analysis of variance on ranks, Dunn test) decrease of bioactivity in the NAB^{high} patients who had MxA expression levels similar to untreated controls, whereas the NAB$^{neg/low}$ patients show clearly sustained bioactivity with increased MxA expression. (B) Absolute MxA values after injection. (C) Ratio of MxA values (MxA after/MxA before IFNβ injection). Analysis of the ratio of MxA values (MxA after/MxA before IFNβ injection) does not yield additional information for discrimination of responders and nonresponders vs absolute MxA values after injection. The lower ratios after/before for Betaferon and Rebif vs Avonex reflect differences of time intervals to previous injection.

we chose a time window of 12 to 24 hours for blood sampling after IFNβ injection.

We observed high positive NAB (>80% neutralizing capacity) in 9, low positive NAB (20 to 80%) in 5, and negative NAB activity (<20%) in 67 patients. Patients with high positive NAB (>80% neutralizing capacity) were distributed as follows: Avonex 0/12, Betaferon 2/18, Rebif 7/52.

High levels of NAB (NAB^{high}) were associated with very low MxA transcription, similar to untreated controls (figure, A; figure E-1 on the *Neurology* Web site at www.neurology.org). Patients with negative and low NAB activity (NAB$^{neg/low}$) had 18-fold higher median MxA levels than untreated controls (figure, A).

We compared RNA extraction immediately after blood drawing and storage of full blood in PAXgene tubes for up to 5 days. The PAXgene system, which greatly simplifies the clinical application, proved to give similar MxA levels as the immediate RNA extraction (data not shown). Analysis of whole blood gave a similar sensitivity to detect IFNβ-mediated induction of MxA as analysis of separated immune cell subsets (monocytes, lymphocytes, neutrophils) (data not shown). Analyzing the after/before ratio of MxA values yielded no additional information compared to the absolute MxA values after injection alone (figure, B and C).

Discussion. Our data confirm that measuring MxA transcription in whole blood offers a practical method for monitoring the bioactivity of all available IFNβ preparations. The method allows reliable identification of NAB^{high} patients. Expression of MxA in NAB$^{neg/low}$ patients was significantly higher than in untreated controls and NAB^{high} patients. A time window between 12 to 24 hours proved to be practical for clinical routine purposes, although a higher induction was seen after 12 hours. MxA induction in NAB^{low} patients demonstrated sustained bioactivity. While other studies used the Kawade[6] method, we applied a simplified NAB CPE assay with results reported in neutralizing capacity. Nevertheless, our results are in full agreement with a recent study[6] clearly demonstrating a decrease of bioactivity in patients with NC above 80%. Thus, in contrast to measuring NAB levels, measuring MxA levels is a straightforward, easy to standardize tool for rating in vivo effects of IFNβ therapy.

From the Institute of Clinical Neuroimmunology (L.A.H., M.K., H.F., T.K., E.M., R.H.), Ludwig-Maximilians-University, Munich; and Marianne-Strauβ-Klinik (M.S., W.P.), Berg, Germany.

Supported by Deutsche Forschungsgemeinschaft DFG (SFB 571), Biogen-Idee and Therapieforschung für Multiple Sklerose Kranke e.V.

Disclosure: R.H. and E.M. have received grant support and consultancy fees from Schering, Teva, Serono, and Biogen-Idec. The other authors report no conflicts of interest.

Received August 11, 2006. Accepted in final form November 27, 2006.

Address correspondence and reprint requests to Prof. Dr. R. Hohlfeld, Institute of Clinical Neuroimmunology, Ludwig-Maximilians-University Munich, Germany, Marchioninistr. 15, 81377 München, Germany; e-mail: reinhard.hohlfeld@med.uni-muenchen.de

References

1. Pachner AR. Measurement of antibodies to interferon beta in patients with multiple sclerosis. Arch Neurol 2001;58:1299–1300.
2. Vartanian TK, Zamvil SS, Fox E, Sorensen PS. Neutralizing antibodies to disease-modifying agents in the treatment of multiple sclerosis. Neurology 2004;63(11 suppl 5):S42–S49.
3. Sorensen PS, Ross C, Clemmesen KM, et al. Clinical importance of neutralising antibodies against interferon beta in patients with relapsing-remitting multiple sclerosis. Lancet 2003;362:1184–1191.
4. Pachner AR, Bertolotto A, Deisenhammer F. Measurement of MxA mRNA or protein as a biomarker of IFNbeta bioactivity: detection of antibody-mediated decreased bioactivity (ADB). Neurology 2003;61(9 suppl 5):S24–S26.
5. Pachner AR, Dail D, Pak E, Narayan K. The importance of measuring IFNbeta bioactivity: monitoring in MS patients and the effect of anti-IFNbeta antibodies. J Neuroimmunol 2005;166:180–188.
6. Pachner AR, Narayan K, Pak E. Multiplex analysis of expression of three IFNbeta-induced genes in antibody-positive MS patients. Neurology 2006;66:444–446.
7. Petersen B, Bendtzen K, Koch-Henriksen N, Ravnborg M, Ross C, Sorensen PS. Danish Multiple Sclerosis Group. Persistence of neutralizing antibodies after discontinuation of IFNbeta therapy in patients with relapsing-remitting multiple sclerosis. Mult Scler 2006;12:247–252.

Phenotypes of female adrenoleukodystrophy

H.H. Jung, MD; I. Wimplinger; S. Jung; K. Landau; A. Gal; and F.L. Heppner

Adrenoleukodystrophy-adrenomyeloneuropathy (ALD-AMN) is an X-linked disorder of the peroxisomal beta oxidation characterized by the accumulation of saturated very long chain fatty acids (VLCFA) predominantly in adrenal cortex and central as well as peripheral myelin.[1] ALD-AMN is caused by mutations of the *ABCD1* gene, a member of the ATP-binding cassette (ABC) transporter superfamily, and more than 400 pathogenic *ABCD1* mutations have been described (www.x-ald.nl).[2]

The incidence of ALD-AMN is estimated to be between 1:20,000 and 1:100,000. Affected men may present with childhood cerebral ALD, adult-onset AMN, or Addison disease only.[1,3] Approximately 20% of heterozygous women develop mild AMN with a mean onset age around 40 years.[1] Childhood onset, cognitive decline, visual disturbances, or adrenal dysfunction are exceptional.[1,3,4]

Herein, we describe two female ALD-AMN heterozygotes presenting with particular cerebral phenotypes, thereby expanding the clinical spectrum of female ALD-AMN and demonstrating a substantial intrafamilial variability.

Case reports. Case 1. This patient was diagnosed with manic-hebephrenic disorder at age 8 years, and had recurrent psychotic episodes thereafter. At age 25 years, neurologic examination revealed spastic paraparesis. Twenty years later, neurologic examination documented moderate cognitive deficits, severe spastic paraparesis, and a cerebellar syndrome with unsteady smooth pursuit gaze movements, dysarthria, and intention tremor. Cerebral MRI showed moderate cerebellar atrophy and pronounced T2 hyperintensities of the cerebellar white matter, but no supratentorial atrophy or signal alterations. In the following years, her condition gradually worsened and she died at age 51 years due to pneumonia.

Autopsy revealed severe demyelination in the cerebral and, considerably more pronounced, the cerebellar white matter (figure). Histologically, cerebellar lesions were gliotic and depleted of axons and oligodendroglia (figure, A, C, E, and G). Cerebral lesions presented with clusters of foamy macrophages harboring myelin and reactive, often gemistocytic astrocytes (figure, B, D, F, and H). While adrenal glands macroscopically appeared normal, histologic examination revealed numerous adrenocortical cells with lamellar eosinophilic cytoplasmic inclusions (figure, I and J).

Her brother was diagnosed with Addison disease at age 47 years. He developed progressive spastic paraparesis and polyneuropathy in his sixth decade. Electroneuromyography showed demyelinating polyneuropathy. Cognitive testing and cerebral MRI were normal.

Case 2. At age 35 years, 1 year after her son died from ALD, this patient became unable to run. Walking difficulties increased and she became wheelchair-dependent at age 48 years. Seven years later, she noted progressive bilateral visual loss. Neurologic examination revealed severe spastic tetraparesis and mild polyneuropathy. Cognitive testing was normal. Ophthalmologic examination demonstrated reduced visual acuity (20/40 in the right eye, 20/30 in the left), severe diffuse visual field impairment, and bilateral optic atrophy (OA). Visually evoked potentials demonstrated bilaterally prolonged P100 latencies (142 msec in the right eye, 135 msec in the left, normal <118 msec). Cerebral MRI revealed bilateral parietooccipital T2 hyperintensities (not shown).

Molecular genetic analysis. DNA was extracted from paraffin-embedded tissue (Patient 1) or from whole blood (Patient 2). The 10 exons of the *ABCD1* gene were amplified, mutation screening was performed with single stranded DNA conformation sensitive (SSCP) electrophoresis, and exons with abnormal SSCP conformers were sequenced. In the brother of Patient 1, a point mutation in exon 7 was found (c.1772G>A), predicting replacement of arginine by glutamine (p.R591Q). Direct sequencing confirmed heterozygosity in Patient 1. In Patient 2, a heterozygous point mutation in exon 2 was found (c.1039C>G), predicting replacement of proline by arginine (p.P218R).

The methylation pattern at the androgen receptor (AR) locus was examined as previously described with minor modifications.[5] In Patient 1, moderately skewed patterns with values of 65:35 (liver) and 82:18 (kidney) were seen. Patient 2 demonstrated a highly skewed X-inactivation with a ratio of 96:4.

Discussion. Both patients had adult-onset AMN, confirming that spastic paraparesis represents the core feature in female ALD-AMN. However, our observations emphasize a possibly earlier onset and broader phenotypic spectrum. The first patient had a childhood-onset psychiatric disorder and adult-onset olivopontocerebellar syndrome due to predominant cerebellar involvement. Similar manifestations are known in male ALD-AMN, but are exceptional in manifesting heterozygous women.[1,3,6] The second patient had late-onset optic atrophy, which has formerly been described only in male childhood-onset ALD. Since the brother of the first patient had Addison disease and late-onset AMN, our observations also document a remarkable intrafamilial phenotypic variability.

Highly skewed X-inactivation was observed in one third of symptomatic female ALD-AMN patients but not in asymptomatic mutation carriers.[4,7] Skewing of X-inactivation was therefore proposed to correlate with clinical severity in ALD-AMN carriers.[7] We found a significantly skewed X-inactivation in the second patient, whereas the first patient had only moderately skewing in liver and kidney tissue. Although the sample origin might influence the degree of X-inactivation, additional genetic or environmental factors have to be postulated to explain the phenotypic variability of female ALD-AMN.

Our observations illustrate and broaden the phenotypic spectrum of manifesting female ALD-AMN carriers and underline the importance to consider female ALD-AMN in the differential diagnosis of various neurologic disorders.

From the Department of Neurology (H.H.J.), Institute of Neuropathology (S.J., F.L.H.), and Department of Ophthalmology (K.L.), University Hospital Zurich, Switzerland; and Institute of Human Genetics (I.W., A.G.), University Medical Center Hamburg-Eppendorf, Hamburg, Germany.

Disclosure: The authors report no conflicts of interest.

Received September 1, 2006. Accepted in final form November 27, 2006.

Address correspondence and reprint requests to Dr. Hans H. Jung, Department of Neurology, University Hospital Zürich, Frauenklinikstrasse 26, 8091 Zürich, Switzerland; e-mail: hans.jung@usz.ch

References

1. Moser HW. Adrenoleukodystrophy: phenotype, genetics, pathogenesis and therapy. Brain 1997;120:1485–1508.
2. Mosser J, Douar AM, Sarde CO, et al. Putative X-linked adrenoleukodystrophy gene shares unexpected homology with ABC transporters. Nature 1993;361:726–730.
3. Moser HW, Raymond GV, Dubey P. Adrenoleukodystrophy: new approaches to a neurodegenerative disease. JAMA 2005;294:3131–3134.
4. Heffungs W, Hameister H, Ropers HH. Addison disease and cerebral sclerosis in an apparently heterozygous girl: evidence for inactivation of the adrenoleukodystrophy locus. Clin Genet 1980;18:184–188.
5. Allen RC, Zoghbi HY, Moseley AB, Rosenblatt HM, Belmont JW. Methylation of HpaII and HhaI sites near the polymorphic CAG repeat in the human androgen-receptor gene correlates with X chromosome inactivation. Am J Hum Genet 1992;51:1229–1239.
6. Marsden CD, Obeso JA, Lang AE. Adrenoleukomyeloneuropathy presenting as spinocerebellar degeneration. Neurology 1982;32:1031–1032.
7. Maier EM, Kammerer S, Muntau AC, Wichers M, Braun A, Roscher AA. Symptoms in carriers of adrenoleukodystrophy relate to skewed X inactivation. Ann Neurol 2002;52:683–688.

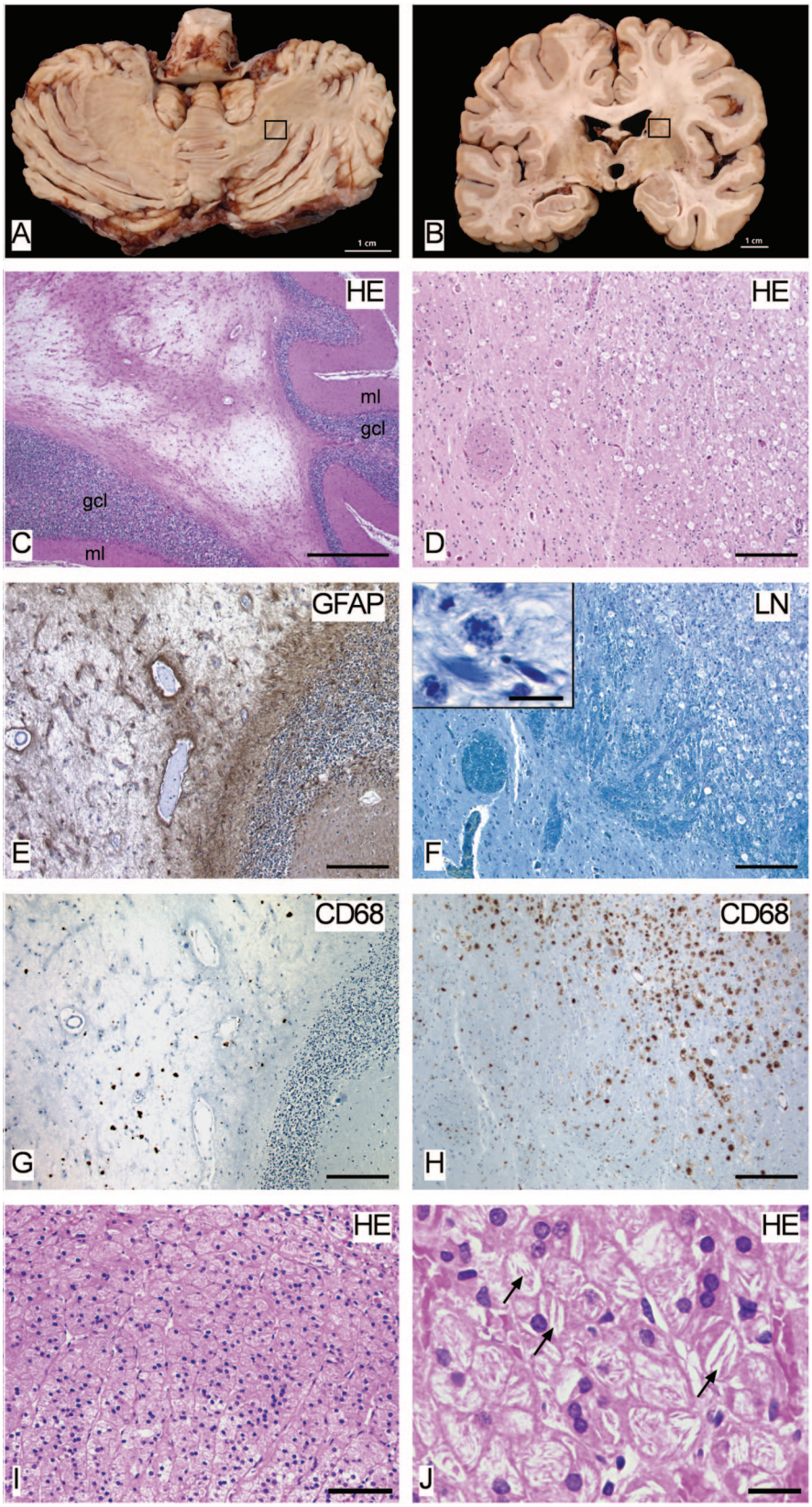

Figure. Brain autopsy: coronal sections of the cerebellum (A) and the cerebrum (B) of Patient 1 depict sharply demarcated white matter lesions. Areas in A and B indicate the corresponding microscopic regions. White matter lesions in the cerebellum were extensive, partially microcystic, did not affect the molecular and granular cell layers (ml and gcl; hematoxylin and eosin, HE; C), and were strongly gliotic as demonstrated by positivity for glial fibrillary acidic protein (GFAP; E). Only few residual CD68$^+$ macrophages remained in these lesions (G). Cerebral lesions located in the basal ganglia presented with rather fresh and CD68$^+$ foamy macrophage-rich lesions restricted to the white matter (HE, D; Luxol-Nissl, LN, F; CD68, H). Foamy macrophages presented as myelinophages harboring myelin (insert in F, spotted blue material inside foamy macrophages). Adrenal gland: Microscopic appearance of Patient's one adrenal gland revealed striated adrenocortical cells (I) containing lamellar eosinophilic cytoplasmic inclusions (arrows in J); while ballooned cells were not visible (HE, I and J). Scale bars: A and B: 1 cm; C: 1 mm; D through I: 200 μm; insert in F and J: 20 μm.

Homozygous mutation in *MYH7* in myosin storage myopathy and cardiomyopathy

Homa Tajsharghi, PhD; Anders Oldfors, MD, PhD; Dominic P. Macleod, MB; and Michael Swash, MD

Myosin storage myopathy (MSM) associated with mutations in *MYH7* encoding for slow/β-cardiac myosin heavy chain (MyHC) occurs sporadically or shows autosomal dominant inheritance.[1-4] MSM is usually associated with severe skeletal muscle weakness, but cardiomyopathy is typically not present. We describe a patient with MSM in whom there was a homozygous mutation (Glu1,883Lys) in *MYH7*. The parents were second cousins, and three of their children developed progressive MSM with respiratory muscle weakness and hypertrophic cardiomyopathy.

Clinical data. This British family consisted of four siblings, three of whom were affected; the parents were second cousins. There was no family history of muscle weakness. The father died with a stroke at age 58 and the mother with myocardial infarct at age 70.

Case 1. Exertional dyspnea commenced in late adolescence for this patient. She presented at age 26 in heart failure, with elevated jugular venous pressure (8 cm), soft systolic murmur at the left sternal edge, and fourth heart sound. She was short (height 141 cm), with thoracic scoliosis. Lung function tests revealed a restrictive deficit. EKG showed right bundle branch block, right axis deviation, and sinus tachycardia. Echocardiography and cardiac catheterization revealed hypertrophic, nonobstructive cardiomyopathy with elevated right ventricular pressure (40 mm Hg systolic) and a restrictive right and left ventricular pattern. Five years later, she developed an acute supraventricular dysrthythmia. Examination at age 34 revealed symmetric limb-girdle weakness and wasting, with mild calf hypertrophy, without myotonia. The blood creatine kinase (CK) level was 161 IU/L (normal < 50 IU/L). Electromyography revealed myopathic motor units. A deltoid muscle biopsy was taken. Her muscle weakness progressed, and by age 45 she was wheelchair dependent. She developed hypercapnic respiratory and cardiac failure requiring nocturnal volume-cycled nasal ventilatory support, with anti-arrhythmic and diuretic therapy. She died at age 57 in cardiorespiratory failure.

Case 2. The younger brother of Case 1 presented at age 25 in acute pulmonary edema following general anesthesia after a traumatic fracture. There was a history of daytime somnolence and headache, with exertional dyspnea. Examination revealed short stature, mild thoracic scoliosis, and mild proximal weakness and wasting. The CK level was 201 IU/L (normal < 160 IU/L). Investigation revealed biventricular hypertrophic cardiomyopathy. He died at age 32 from cardiac failure.

Case 3. This brother presented at age 44 with daytime somnolence, leg weakness, and hypercapnic respiratory failure, requiring urgent tracheotomy and ventilatory support. He was of short stature (height 155 cm), with a myopathic facies, a high-arched palate, thoracic scoliosis, a weak sniff test, and proximal muscle weakness and wasting, but no myotonia. The CK level was >3,000 IU/L (normal < 160 IU/L). Investigation revealed biventricular hypertrophic cardiomyopathy and heart failure. He was managed with nasal positive pressure ventilation and diuretic therapy. A biceps brachii muscle biopsy was performed.

Muscle biopsy findings. Muscle samples from the three siblings showed similar findings typical for MSM. Hyaline bodies were seen in type 1 fibers, but not in type 2 fibers, consisting of amorphous eosinophilic material, faintly green in Gomori trichrome, negative in oxidative enzyme preparations and periodic acid–Schiff, but faintly positive in ATPase preincubated at pH 4.3. Immunostains for titin, nebulin, and α-actinin were negative. Electron microscopy revealed moderately electron-dense, nonfilamentous, finely granular amorphous material that seemed to infiltrate myofibrils. Cardiac muscle from Case 2 at autopsy showed fibrosis, loss of myocytes, and hyaline bodies in remaining myocytes.

Genetic findings. The entire coding sequence of *MYH7* in genomic DNA was sequenced in Case 3.[1] We identified a homozygous missense mutation in exon 38 (24,012G→A), changing the highly conserved and negatively charged glutamate at position 1,883 to the positively charged lysine (figure E-1 on the *Neurology* Web site [www.neurology.org]). The Glu1,883Lys mutation is located in the distal end of the filament forming rod region of slow/β-cardiac MyHC, in the 29-residue assembly-competence domain (1,871 to 1,899), which is essential for filament assembly[5] (figure E-1).

Accession numbers were for genomic *MYH7* sequence aj238393 and for cDNA *MYH7* sequence m58018.

Discussion. This family with MSM presented with type II respiratory failure and cardiac failure, due to hypertrophic cardiomyopathy, associated with a homozygous mutation in the distal rod region of slow/β-cardiac MyHC. The mode of inheritance differs from previously described patients with MSM and *MYH7* mutations. The parents were unaffected second cousins. The investigated sibling was homozygous for the mutation, suggesting autosomal recessive inheritance. The previously reported cases with MSM associated with *MYH7* mutations were heterozygous for the mutation, and dominant inheritance was demonstrated for these mutations. Previously reported patients with dominantly inherited MSM associated with *MYH7* mutations have not developed cardiomyopathy or type II respiratory failure, suggesting that the phenotypes of recessively and dominantly inherited cases differ. The majority of *MYH7* mutations are dominant and associated with cardiomyopathy, but there are reported examples of mutations in *MYH7*, without skeletal myopathy, causing severe cardiomyopathy in homozygotes but only mild or no signs of cardiomyopathy in heterozygotes.[6] In the family with MSM reported here, genetic analysis could only be performed in Case 3, and therefore we cannot rule out heterozygosity in the other siblings.

Although previously reported patients with MSM associated with different *MYH7* mutations did not show cardiomyopathy, this is not unique, as in Laing early-onset distal myopathy, caused by mutations in another region of *MYH7*, cardiac involvement is absent.[7]

As in previously reported patients with MSM, the mutated residue is located in a b-, f-, or c-position in the coiled-coil structure of the distal rod region of the MyHC dimer (figure E-1). Residues in these positions may interact with other MyHC dimers or myosin binding proteins, explaining why mutations affecting such residues can cause defective assembly of thick filaments. The previously reported cases were all heterozygous for the mutation, whereas our Case 3 was homozygous. The parents were second cousins and therefore probably unaffected heterozygous carriers of the mutation, indicating that the Glu1,883Lys mutation is less pathogenic in recessive form than the previously reported *MYH7* mutations associated with MSM. Our findings suggest that the mutated residue Glu1,883, which is located within the assembly-competence domain of the MyHC,[5] is important for thick filament assembly both in skeletal and in cardiac muscle.

From the Department of Pathology (H.T., A.O.), Sahlgrenska University Hospital, Goteborg, Sweden; and Departments of Respiratory Medicine (D.P.M.), and Neurology (M.S.), Royal London Hospital, UK.

Supported by grants from the Swedish Research Council (project no. 07122) and the Association Francaise Contre les Myopathies.

Disclosure: The authors report no conflicts of interest.

Received August 31, 2006. Accepted in final form November 30, 3006.

Address correspondence and reprint requests to Dr. A. Oldfors, Department of Pathology, Sahlgrenska University Hospital, SE-413 45 Goteborg, Sweden; e-mail: anders.oldfors@gu.se

Additional material related to this article can be found on the *Neurology* Web site. Go to www.neurology.org and scroll down the Table of Contents for the March 20 issue to find the title link for this article.

References

1. Tajsharghi H, Thornell LE, Lindberg C, et al. Myosin storage myopathy associated with a heterozygous missense mutation in MYH7. Ann Neurol 2003;54:494–500.
2. Bohlega S, Abu-Amero SN, Wakil SM, et al. Mutation of the slow myosin heavy chain rod domain underlies hyaline body myopathy. Neurology 2004;62:1518–1521.
3. Laing NG, Ceuterick-de Groote C, Dye DE, et al. Myosin storage myopathy: slow skeletal myosin (MYH7) mutation in two isolated cases. Neurology 2005;64:527–529.
4. Dye DE, Azzarelli B, Goebel HH, Laing NG. Novel slow-skeletal myosin (MYH7) mutation in the original myosin storage myopathy kindred. Neuromusc Disord 2006;16:357–360.
5. Sohn RL, Vikstrom KL, Strauss M, et al. A 29 residue region of the sarcomeric myosin rod is necessary for filament formation. J Mol Biol 1997;266:317–330.
6. Richard P, Charron P, Leclercq C, et al. Homozygotes for a R869G mutation in the beta-myosin heavy chain gene have a severe form of familial hypertrophic cardiomyopathy. J Mol Cell Cardiol 2000;32:1575–1583.
7. Meredith C, Herrmann R, Parry C, et al. Mutations in the slow skeletal muscle fiber myosin chain gene (MYH7) cause Laing early-onset distal myopathy (MPD1). Am J Hum Genet 2004;75:703–708.